PHYSICS INFORMED GUIDED DIFFUSION FOR ACCELERATED MULTI-PARAMETRIC MRI RECONSTRUCTION

Perla Mayo*, Carolin M. Pirkl‡, Alin Achim*, Bjoern Menze**, and Mohammad Golbabaee*

* University of Bristol | ‡GE Healthcare | **University of Zurich

MOTIVATION

Reconstruction of high quality multiparametric MRI e.g., Magnetic Resonance Fingerprinting (MRF)[1] from highly-accelerated acquisitions.

Challenges: Severely aliased/corrupted inputs / high computational cost of Denoising Diffusion Models (DDM[2,3,4]) / adherence to the acquisition physics.

MRF-DiPh

- MRF reconstruction problem:

$$\arg\min_{\mathbf{x}\in\mathcal{B}} f(\mathbf{x}) + \lambda h(\mathbf{x}) \qquad (1)$$

  - $\mathbf{x}$: MRF images to reconstruct
  - $f(\mathbf{x}) = ||\mathbf{y} - \mathbf{A}\mathbf{x}||_2^2$ k-space consistency w/ measurements $\mathbf{y}$, given forward operator $\mathbf{A}$
  - $h(\mathbf{x})$ regularizer/image prior
  - $\boldsymbol{\mathcal{B}} \coloneqq \{\mathbf{x} \;\text{ s.t. }\; \mathbf{x} = \boldsymbol{\rho} \cdot D(\mathbf{T1}, \mathbf{T2})\}$ Bloch model consistency w/ tissue maps $\mathbf{T1}, \mathbf{T2}$ and proton density ($\boldsymbol{\rho}$) via MRF dictionary D
- Formulates Eq. (1) as a HQS problem with a DDM prior[5].
- Solves following ADMM (Algorithm 1)
- Outputs reconstructed MRF images $\mathbf{x}_{rec}$ and parameter maps $\mathbf{q}_{rec}$.

SOLUTION: OUR CONTRIBUTION

MRF-DiPh, an MRF reconstruction method:

- based on DDM approaches
- conditioned on low-quality reconstructions
- guided at sampling by the physics of the model by
  - k-space (measurement) consistency
  - Bloch equations

Algorithm 1 MRF-DiPh

Require: $f, \epsilon_\theta, \{t_k\}_{k=1}^K, \{\bar{\alpha}_{t_k}\}_{k=1}^K, \lambda, \tau, \xi$

1: Set $\sigma_k^2 \coloneqq (1-\bar{\alpha}_{t_k})/\bar{\alpha}_{t_k}, \mu_k \coloneqq \lambda/\sigma_k^2, \gamma_k \coloneqq \tau\mu_k$
2: Initialize $\mathbf{x}_K \sim \mathcal{N}(\mathbf{0}, \mathbf{Id}), \mathbf{z}_K = \mathbf{v}_K = 0$
3: **for** $k = K, \ldots, 1$ **do**
4: $\quad \tilde{\mathbf{x}}_{0,k} = (1/\sqrt{\bar{\alpha}_{t_k}})\,(\mathbf{x}_k - \sqrt{1-\bar{\alpha}_{t_k}}\epsilon_\theta(\mathbf{x}_k, t_k, \mathbf{x}_c))$
5: $\quad \hat{\mathbf{x}}_{0,k} = prox_{\frac{1}{\mu_k+\gamma_k}f}\left(\frac{\mu_k\tilde{\mathbf{x}}_{0,k}+\gamma_k\mathbf{z}_k-\mathbf{v}_k}{\mu_k+\gamma_k}\right)$
6: $\quad (\mathbf{z}_{k-1}, \mathbf{q}_{k-1}) \leftarrow \mathrm{DICT{-}MATCH}(\hat{\mathbf{x}}_{0,k} + \mathbf{v}_k/\gamma_k)$
7: $\quad \mathbf{v}_{k-1} = \mathbf{v}_k + \gamma_k(\hat{\mathbf{x}}_{0,k} - \mathbf{z}_{k-1})$
8: $\quad \hat{\epsilon}_k = (1/\sqrt{1-\bar{\alpha}_{t_k}})\,(\mathbf{x}_k - \sqrt{\bar{\alpha}_{t_k}}\mathbf{z}_{k-1})$
9: $\quad \epsilon \sim \mathcal{N}(\mathbf{0}, \mathbf{Id})$
10: $\quad \mathbf{x}_{k-1} = \sqrt{\bar{\alpha}_{t_{k-1}}}\mathbf{z}_{k-1} + \sqrt{1-\bar{\alpha}_{t_{k-1}}}(\sqrt{\xi}\boldsymbol{\epsilon} + \sqrt{1-\xi}\hat{\boldsymbol{\epsilon}}_k)$
11: **end for; return** $\mathbf{x}_{rec} = \mathbf{z}_0, \mathbf{q}_{rec} = \mathbf{q}_0 \coloneqq \{\mathbf{T1}_0, \mathbf{T2}_0, \boldsymbol{\rho}_0\}$

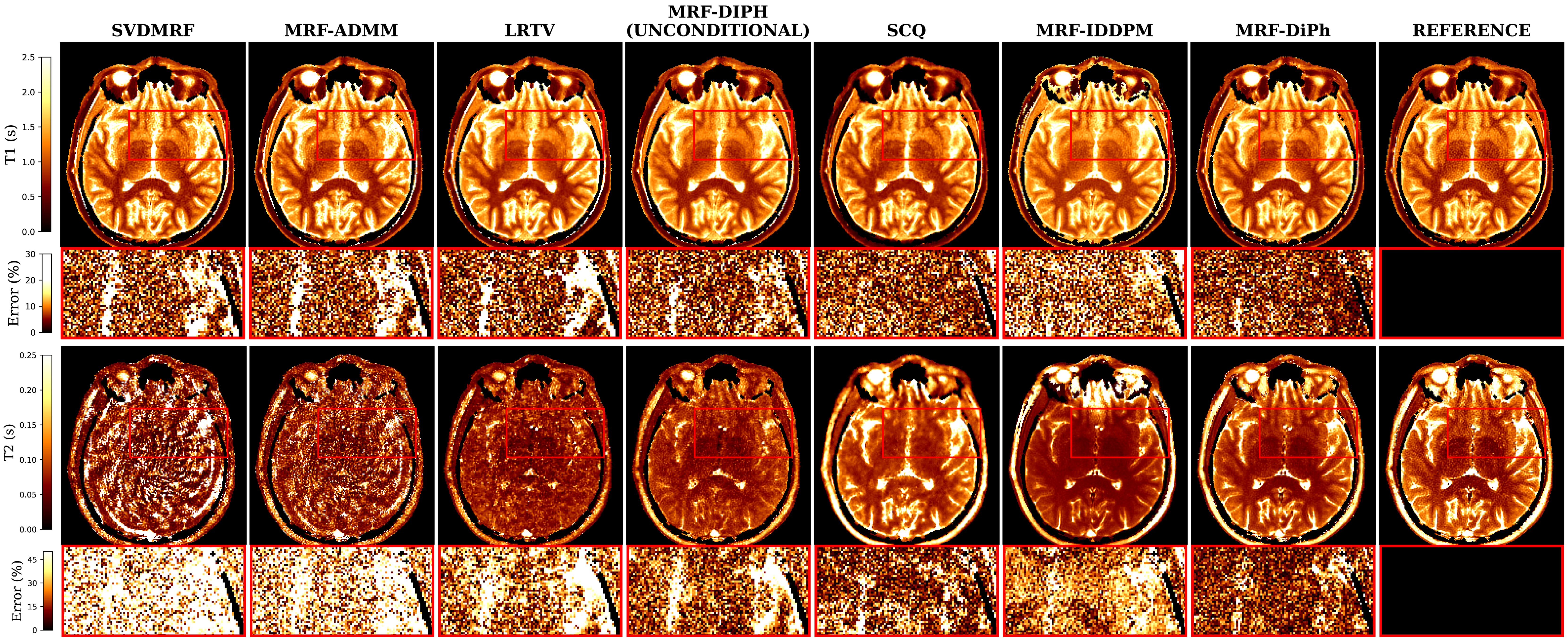

Figure 1. Reconstructions of T1 and T2 maps for the assessed approaches on data with acceleration factor of 5

Table 1. *Metrics for reconstructions of T1/T2 maps from accelerated k-space data (R=5)*

Method	MAPE (%)		NRMSE	
	T1	T2	TSMI	k-space
SVDMRF	20.01	144.27	57.10	99.93
MRF-ADMM	20.30	68.51	30.90	18.69
LRTV	19.84	39.01	37.95	11.72
SCQ	8.76	22.61	--	--
MRF-IDDPM	8.45	22.54	27.26	36.06
MRF-DiPh (base)	**6.75**	**18.40**	**18.65**	**22.82**
MRF-DiPh (A)	6.80	18.41	18.70	22.52
MRF-DiPh (B)	7.15	18.63	18.64	22.40
MRF-DiPh (C)	7.17	18.82	18.79	22.12
MRF-DiPh (D)	11.32	29.78	25.36	19.17

Table 2. *MRF-DiPh reconstruction time vs. accuracy for various sampling steps (K) and maximum CG iterations. Results are for test image in Figure 1.*

MRF-DiPh	Base	K				CG		
		5	10	20	50	1	10	20
Runtime (s)	44.17	8.83	15.88	30.03	72.29	30.02	61.03	91.79
TSMI NRMSE	15.76	16.74	14.99	15.55	16.06	15.73	15.87	15.70
(T1 + T2)/2 MAPE	10.42	14.20	11.93	10.62	10.22	10.37	10.45	10.33

NUMERICAL EXPERIMENTS

- 8 subjects, 15 axial slices each (train/test split = 75%/25%)
- Acceleration factor R=5 simulated on k-space
- Reference from unaccelerated, densely-sampled acquisitions
- Benchmarks: SVDMRF[6], MRF-ADMM[7], LRTV[8], SCQ[9], and MRF-IDDPM[10]
- Ablation studies: $\xi = 0.5$ (**mode A**), $\xi = 0.0$ (**mode B**), MRF-DiPh w/o DICT−MATCH (**mode C**) and unconditional DDM w/ physics guidance (**mode D**)

RESULTS & DISCUSSION

- **MRF-DiPh** ★★★★★ | MRF-IDDPM★★★☆☆ | CNN★★☆☆☆ | LRTV ★☆☆☆☆ | MRF-ADMM ★☆☆☆☆ | SVDMRF ☆☆☆☆☆
- MRF-DiPh:
  - = lower errors (Tab. 1) + more defined anatomies (Fig. 1)
  - >> MRF-DiPh w/o DICT−MATCH (Mode C).
- Data-driven >> Unconditional MRF-DIPh (Mode D) >> Classical
- ↓errors + ↑reliability = DDM prior + Physics Guidance = MRF-DiPh

REFERENCES

1. D. Ma et al., Nature, 2013; **2.** Ho et al., Advances in Neural Information Processing Systems, 2020; **3.** Nichol et al., International Conference in Machine Learning, 2021; **4.** Dhariwal and Nichol, Advances in Neural Information Processing Systems, 2021; **5.** Boyd et al., Foundations and Trends© in Machine Learning, 2011; **6.** D. McGivney, et al. IEEE transactions on medical imaging, 2014; **7.** Asslander et al., Magnetic Resonance in Medicine, 2018; **8.** Golbabaee et al., Medical Image Analysis, 2021; **9.** Fang et al., IEEE Transactions on Medical Imaging, 2019; **10.** Mayo et al. arXiv preprint, 2024;